Quantifying the Dynamic Ocean Surface Using Underwater Radiometric Measurement

Lian Shen
Department of Mechanical Engineering
& St. Anthony Falls Laboratory
University of Minnesota
Minneapolis, MN, 55455
phone: (612) 625-7527 fax: (612) 624-5230 email: shen@umn.edu

Award Number: N00014-13-1-0370

LONG-TERM GOALS

The primary focuses of this research are to understand the requirements of the inverse modeling of sea-surface processes on the accuracy, resolution, and coverage of underwater unpolarized and polarized light-field measurements, to master the theoretical constraints and computational resources required of the modeling and simulation, and to improve the forward theoretical and simulation prediction capabilities in terms of accuracy and efficiency. We aim to investigate the feasibility and limitations of achieving the inverse problem of modeling the ocean surface using underwater light measurements. Our ultimate goal is to establish an efficacious, robust framework for the unique and efficient solution of the inverse problem in terms of both the statistical characterization and direct phase-resolved prediction of the ocean surface.

OBJECTIVES

The scientific and technical objectives of our research are to:

- develop numerical capabilities for the large-eddy simulation (LES) of the dynamically-coupled wind-wave-turbulence flows and surface roughness
- develop parameterization modeling of key effects of the dynamical ocean surface on the underwater light patterns and statistics
- develop highly computationally-efficient Monte Carlo radiative transfer (RT) modeling and a semi-analytical model for Green function of 3-D RT equation
- develop a computational framework of the inverse problem for ocean waves and upper ocean vortical flows using under water radiance data
- use computational tools for the inverse problem to model key flow processes at the sea surface based on underwater light measurement and to quantify the feasibility requirements and limits on applicability of the inverse problem

Report Documentation Page

Form Approved
OMB No. 0704-0188

1. REPORT DATE	2. REPORT TYPE	3. DATES COVERED
30 SEP 2013		**00-00-2013 to 00-00-2013**

4. TITLE AND SUBTITLE	5a. CONTRACT NUMBER
Quantifying the Dynamic Ocean Surface Using Underwater Radiometric Measurement	5b. GRANT NUMBER
	5c. PROGRAM ELEMENT NUMBER
6. AUTHOR(S)	5d. PROJECT NUMBER
	5e. TASK NUMBER
	5f. WORK UNIT NUMBER
7. PERFORMING ORGANIZATION NAME(S) AND ADDRESS(ES) **University of Minnesota,Department of Mechanical Engineering & St. Anthony Falls Laboratory,Minneapolis,MN,55455**	8. PERFORMING ORGANIZATION REPORT NUMBER
9. SPONSORING/MONITORING AGENCY NAME(S) AND ADDRESS(ES)	10. SPONSOR/MONITOR'S ACRONYM(S)
	11. SPONSOR/MONITOR'S REPORT NUMBER(S)

12. DISTRIBUTION/AVAILABILITY STATEMENT
Approved for public release; distribution unlimited

13. SUPPLEMENTARY NOTES

14. ABSTRACT

15. SUBJECT TERMS

16. SECURITY CLASSIFICATION OF:			17. LIMITATION OF ABSTRACT	18. NUMBER OF PAGES	19a. NAME OF RESPONSIBLE PERSON
a. REPORT **unclassified**	b. ABSTRACT **unclassified**	c. THIS PAGE **unclassified**	**Same as Report (SAR)**	**11**	

APPROACH

We develop a suite of comprehensive, efficient, and physical-based numerical tools for the simulations of ocean waves, turbulence, and radiance transfer, and the data assimilation capability of ocean waves. The simulation of ocean waves and turbulence is coupled with the calculation of radiance transfer and the inverse modeling of data assimilation.

For the dynamical evolution of nonlinear ocean waves, we employ a computational tool called simulation of nonlinear ocean waves (SNOW), which is an accurate and efficient tool for the nonlinear wave simulation in a phase-resolved framework. The SNOW simulates nonlinear waves based on Zakharov equation using a pseudo-spectral method. The SNOW is capable to resolve nonlinear wave-wave interactions to any desired perturbation order. We have also included the wave-breaking dissipation model and the wind forcing directly through the coupling with wind simulation to the SNOW. Such simulation will provide detailed spatial and temporal information of broadband waves in realistic ocean environment.

In addition to ocean waves, surface roughness associated with turbulent flow and wind also strongly affects the radiative transfer at ocean surface. In this study, we perform LES to simulate the turbulent flow in the upper ocean under the ocean waves as well as wind above waves. In our LES, three-way interactions among wind, wave, and turbulence are captured. The governing equations for the resolved turbulence eddies are the filtered Navier-Stokes equations. An advanced scale-dependent Lagrangian dynamic model for subgrid-scale (SGS) is used. At the sea surface, a promising model proposed by PI's group is employed to dynamically address the sea-surface roughness effect without empirical tuning of model coefficient. For surface wave with moderate slope, an accurate simulation with boundary-fitted grid is used. The nonlinear viscous kinematic and dynamic boundary conditions are applied at the free surface. For steep and breaking surface waves and air-water mixed flow, a hybrid multi-fluids simulation is performed on a fixed Eulerian grid. The multi-fluids flow simulation combines the strengths of level-set, volume-of-fluid, and ghost fluid methods. Such turbulent flow simulation will provide modeling of sea-surface roughness.

We have developed three-dimensional forward unpolarized and polarized Monte Carlo (MC) models to simulate the light propagation in the inhomogeneous upper ocean subject to Snell's law, Fresnel transmission, scattering, and absorption. The instantaneous surface geometry is obtained in the SNOW and ocean turbulent flow simulation. When photons travel in sea, they are affected by the light absorption and scattering effects in water. In the unpolarized MC simulation, the photon traveling distance, scattered polar angle, and azimuthal angle are determined stochastically. Finally, radiance is quantified through the statistics of the photons. To consider the polarized light process, we have also developed numerical tools to simulate the vector RT equation. In the polarized RT simulation, photon traveling path length, source function, and scattering angle is chosen based on several biased sampling techniques to reduce the variance of the results and account for the Mie scattering. Our code is validated by comparing with previous modeling and measurement. The effect of turbulence on the variation of inherent optical properties (IOPs) is also considered. We have developed an extended MC simulation capability with inhomogeneous RT equation with empirical formulations for the dependence of absorption coefficient, scattering coefficient, refractive index, and phase function on a variety of physical quantities such as temperature, salinity, and chlorophyll concentration which are provided by our ocean turbulent flow simulation.

For the inverse modeling, we have developed an efficacious optimization scheme to reconstruct the sea surface based on the RT, wave, and turbulence simulations. We have also developed a framework of data assimilation of surface motion through the adjoint model of 4DVAR. The inverse modeling will play an important role in this project.

To meet the computational challenges of the research in this project, the simulation tools for wave, turbulence, RT, and inverse modeling are developed in the framework of large-scale high-performance computation on parallel computers. The developed codes are parallelized using massage passing interface (MPI) based on domain decomposition.

WORK COMPLETED

During the fiscal year of 2013, substantial progresses have been made. Research performed includes

- Investigation of the dynamical interaction between wave and ocean turbulence in terms of wave flow field, turbulence vorticity, Reynolds stresses, turbulence kinetic energy, and the energy transfer between wave and turbulence in both the wave Eulerian and Lagrangian frames.
- Investigation of turbulence transport mechanism near the free surface and the effect of near-surface turbulence on scalar (e.g., temperature and salinity) transport.
- Development of numerical capability of large-eddy simulation of wind-wave interaction.
- Establishment of an extensive simulation database for wind-forcing waves. Using the surface geometry obtained from wind-wave simulation, a large set of RT simulations has been performed. The effect of wind forcing on the geometry of wave surface and the irradiance field underneath has been studied.
- Investigation of realistic, large-scale ocean waves subject to wind forcing and nonlinear wave-wave interaction and the effect on the underwater irradiance field.

RESULTS

Wave-turbulence interaction affects the geometry of ocean surface, the generation and dissipation of ocean waves, and the transport of scalars (e.g., temperature, salinity, and chlorophyll concentration) near ocean surface. We have investigated the dynamical interaction between wave and ocean turbulence. Figure 1 shows an example of the distortion effect of wave on the evolution of turbulence streamwise vorticity. As shown in figure 1(a), the wave strain field periodically distorts turbulence streamwise vorticity. Turbulence streamwise vorticity is stretched under wave backward slope and is compressed under wave forward slope. Under wave crest and trough, turbulence streamwise vorticity is turned to the counter-clockwise and clockwise directions, respectively. We also found that the effect of turbulence motion on the evolution of turbulence streamwise vorticity is as important as the effect of the wave strain field. Figure 1b shows that turbulence streamwise vorticity is stretched by turbulence motion at all the wave phases near the free surface.

We have also studied the transport mechanism of free surface turbulence and the effect of turbulence on the scalar transport near the free surface. Figure 2shows an example result of surface-connected vortex, which is an important characteristic flow structure of free-surface turbulence and often exists for a long time period. As a surface-connected vortex exists, turbulence motion in the horizontal

directions is transferred to the vertical direction through pressure-strain correlation (figure 2a). The downward motion at the center of the surface-connected vortex also brings a large amount of turbulence energy associated with horizontal motion away from the free surface to the deep region (figure 2b). The transport effect due to pressure moves the turbulence energy associated with the vertical motion away from the free surface (figure 2d), and the transport due to turbulence motion transports the energy further to the deep region (figure 2c). Figure 3 shows an example of conditional averaged flow and scalar fields, with conditional averaging performed with respect to strong vertical vortices. The vertical vortex is accompanied by downwelling motion, as indicated by the downward swirling streamlines. Because of the downwelling motion, the scalar is convected from the near-surface region to the region below. As a result, the scalar surface flux is reduced.

Wind forcing and breaking waves are two important factors affecting the geometry of ocean surface. We have investigated breaking waves under wind forcing and the irradiance under the sea surface. Figure 4 shows an example of the instantaneous wind velocity, breaking surface, and irradiance field captured in the dynamically-coupled wind-wave simulation. Before the wave breaks (figure 4a), the irradiance field is approximately two-dimensional, and irradiance focusing zones are formed under the wave crests. At the early stage of wave breaking (figure 4b), although the irradiance mainly focuses under the wave crest, the variation of the irradiance along the direction of the wave crest increases. Dark zones are identified under the plunging jet at the forward slope of the breaking wave, which is due to the multiple penetrations of light rays cross the air-sea surface. During the wave breaking (figure 4c), as the plunging jet falls onto the forward slope of the wave, a highly turbulent surface is generated. The irradiance focusing under the wave crests becomes weak and the irradiance field is highly three-dimensional. After the wave breaking (figure 4d), the irradiance field becomes completely three-dimensional under the wave field.

Figure 5 shows an example of wind effect on breaking waves and the underlying irradiance field. At low wind speed (figure 5a), the surface and the irradiance field are approximately two-dimensional. The irradiance focusing zone and dark zone clearly appear under the wave crest and the plunging jet at the forward slope of the surface wave, respectively. At intermediate wind speed (figure 5b), the wave crest and plunging jet becomes three dimensional. Water spumes are generated. The variation of the focusing irradiance field along the direction of the wave crest increases. Compared with that in the low wind speed case, the size of the dark zone decreases. At high wind speed (figure 5c), the wave surface and irradiance field become three dimensional. Neither the irradiance focusing zone nor the dark zone is observed.

In addition to the local wind-wave interaction simulation, we have also studied the irradiance field beneath large-scale wave field under the action of winds and nonlinear wave-wave interaction. Figure 6 shows an example result of two ocean wave spectra, i.e., Pierson-Moskowitz spectrum and JONSWAP spectrum. In general, the focusing in the irradiance field under the JONSWAP spectrum is stronger than under the Pierson-Moskowitz spectrum. We also consider the effect of swell on the irradiance field under ocean wave spectrum. As shown, under the swell crest, the surface curvature of the swell leads to a large irradiance focusing zone, whereas under the swell trough, a defocusing zone is generated.

IMPACT/APPLICATIONS

This study aims to obtain a deep understanding of the feasibility and limitations of reverse modeling and to develop the modeling tools to characterize the ocean surface using underwater radiance

measurements. The simulation and modeling tools developed in our research will fundamentally improve the capability of ocean surface reconstruction and the understanding of the correlation between the surface motion and the underwater radiance field. The result of our analysis and modeling is also expected to provide guidance for experimental observation. In our study, various wind-wave conditions are considered, including severe flow conditions, e.g., strong wind blowing over breaking waves, highly mixed air and water, etc. Many of the above processes are difficult to measure directly. With the estabilshment of the simulation database of underwater radiance field under various wind and wave conditions, our study will help to interprete sparse observation datasets. The ultimate application of this project is to provide a framework for the development of underwater-radiance-based surface reconstruction tools for navy operations.

TRANSITIONS

The numerical datasets obtained from this project will provide useful information on physical quantities difficult to measure, and will provide guidance, cross-calibrations, and validations for experiments. This project will also establish a framework and a physical basis to characterize the ocean surface using underwater radiance measurements.

RELATED PROJECTS

This project is performed in collaboration with Professor Dick K.P. Yue's group at MIT who is funded separately.

PUBLICATIONS

Guo, X. & Shen, L. (2013), Numerical study of the effect of surface waves on turbulence underneath. Part 1. Mean flow and turbulence vorticity, *Journal of Fluid Mechanics,* Vol. 733, pp.558-587.

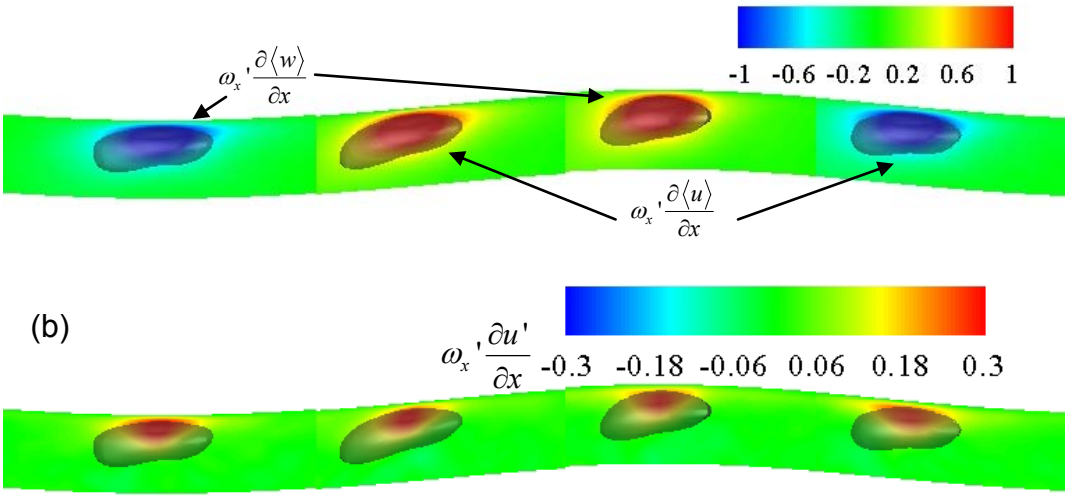

Figure 1. Averaged flow field conditioned upon streamwise vorticity. On the vertical cross-section passing the center of streamwise vorticity, (a) contours of vorticity turning due to wave motion under the wave crest and trough and contours of vorticity stretching due to wave motion under the wave forward and backward slopes and (b) contours of vorticity stretching due to turbulence motion.

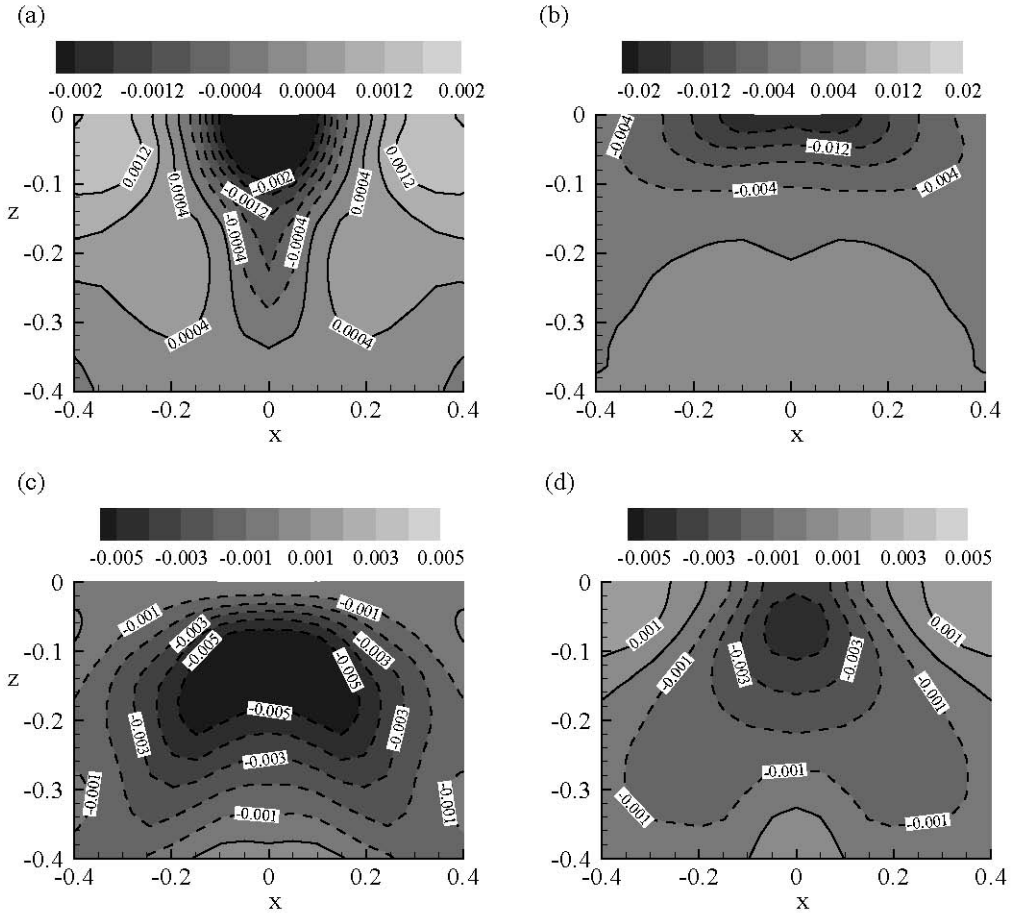

Figure 2. Averaged flow field conditioned upon strong surface-connected vortex. On the vertical cross-section passing the center of surface-connected vorticity, the following are plotted: (a) pressure-strain correlation, (b) turbulent transport of turbulent energy associated with horizontal motion, (c) turbulent transport of turbulent energy associated with vertical motion, and (d) pressure transport.

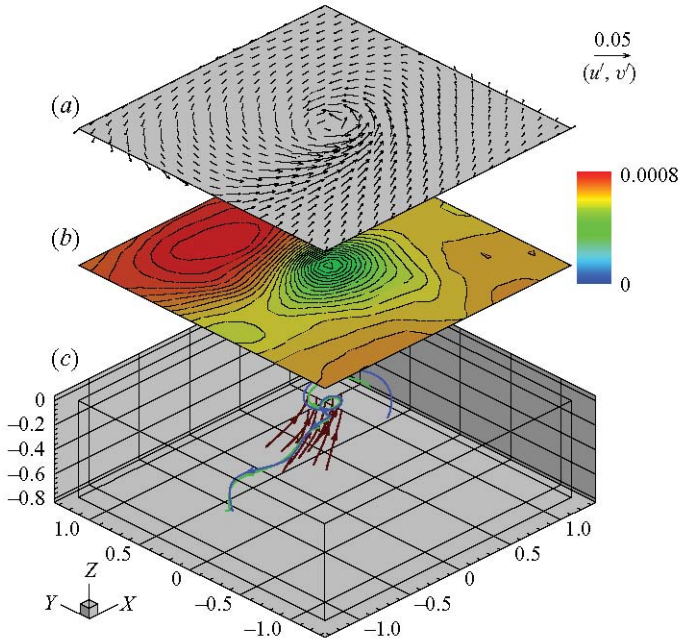

Figure 3. Averaged results of flow and scalar fields conditioned upon strong positive-vertical-vorticity events. The following are plotted: (a) velocity of fluctuating velocity at the surface, (b) contours of scalar flux at the surface, and (c) representative vortex lines (with brown coloar) and streamlines (with the green and blue colors).

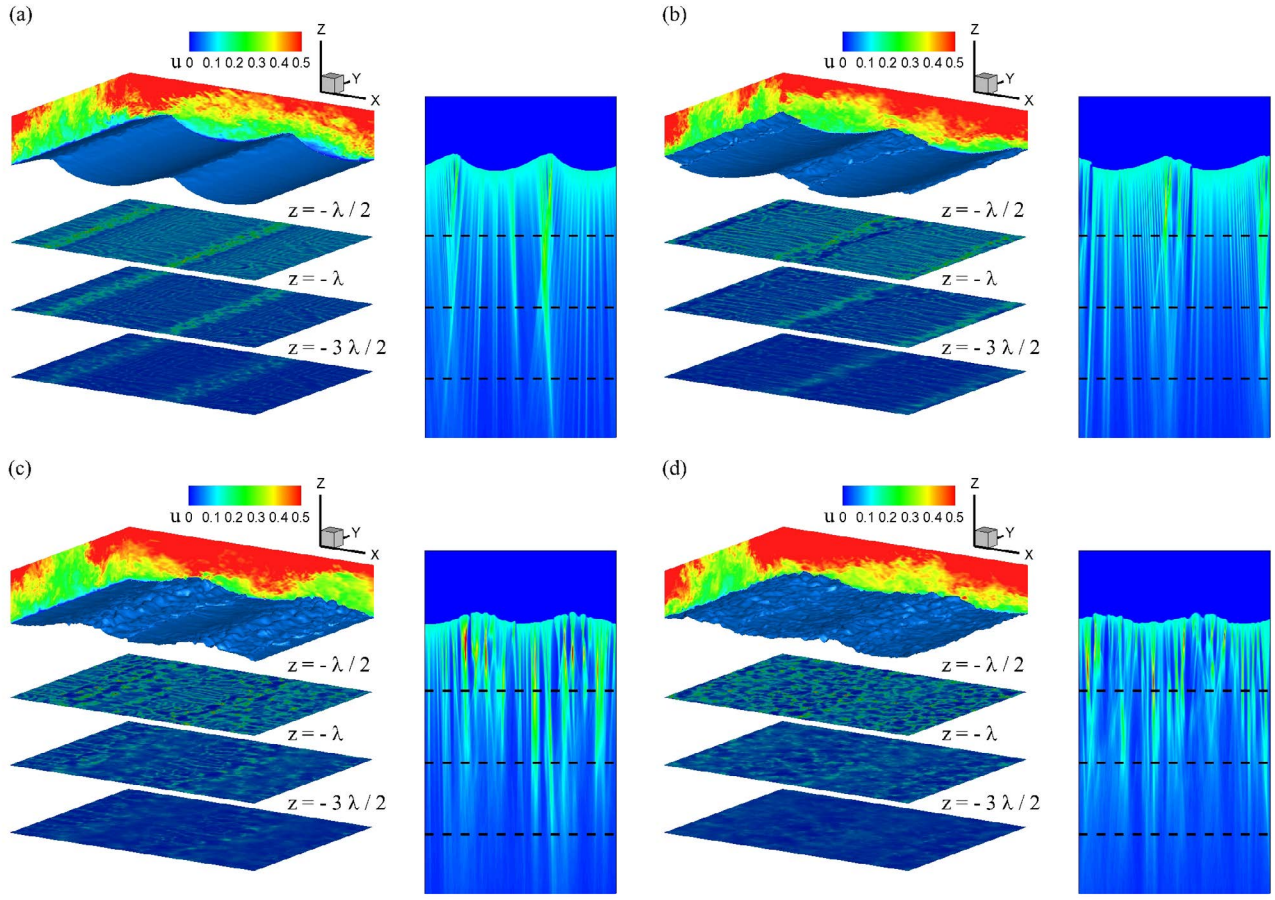

Figure 4. Irradiance field under wind-forcing, breaking waves captured in the wind-wave simulation. The breaking surface profiles, contours of horizontal wind velocity, horizontal distribution of downwelling irradiance field at representative depths, and vertical distribution of downwelling irradiance field across the breaking surface are shown (a) before, (b) at the early stage of, (c) during, and (d) after wave breaking.

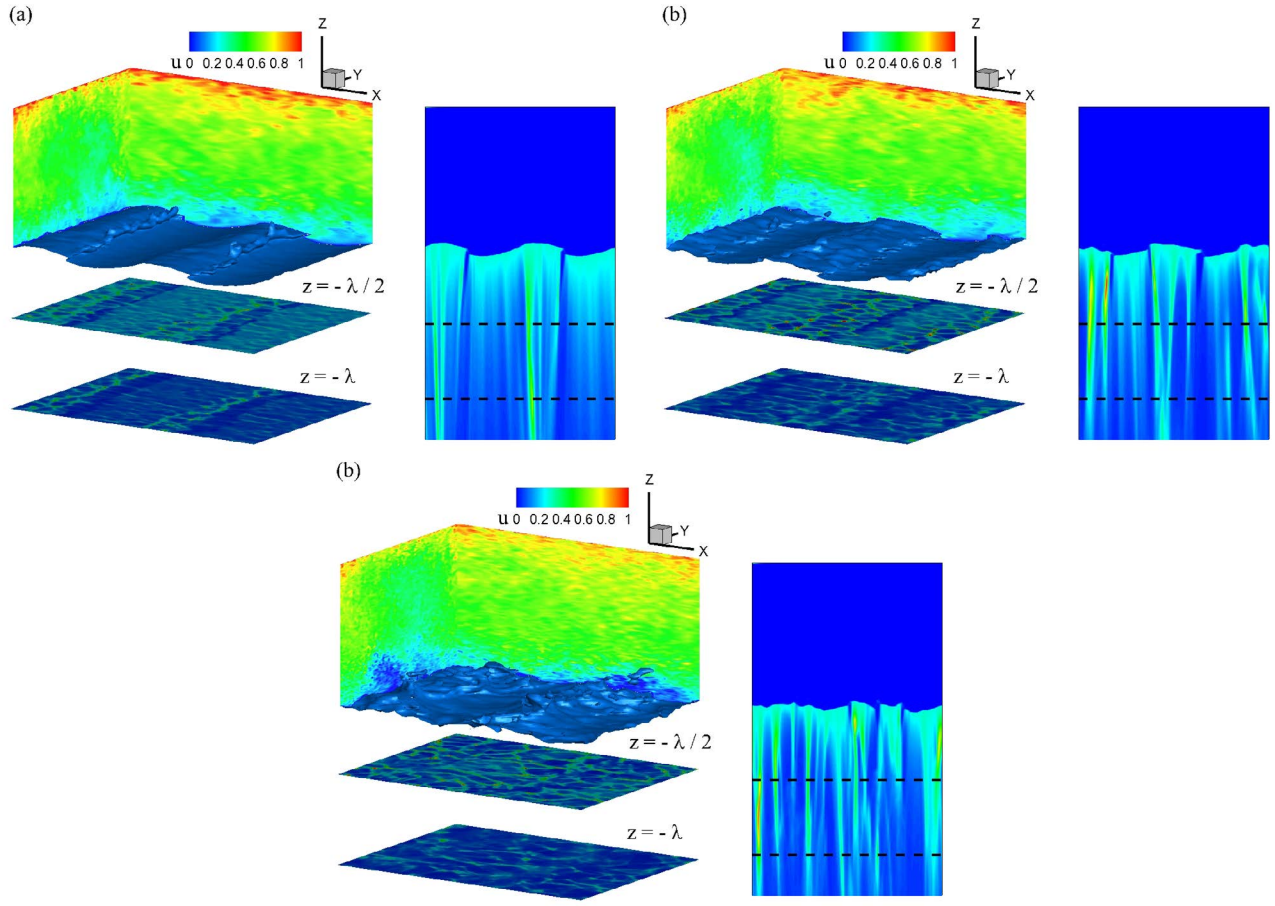

Figure 5. Irradiance field under wind-forcing, breaking waves captured in the wind-wave simulation. The breaking surface profiles, contours of horizontal wind velocity, horizontal distribution of downwelling irradiance field at representative depths, and vertical distribution of downwelling irradiance field across the breaking surface are shown at (a) low, (b) intermediate, and (c) high winds.

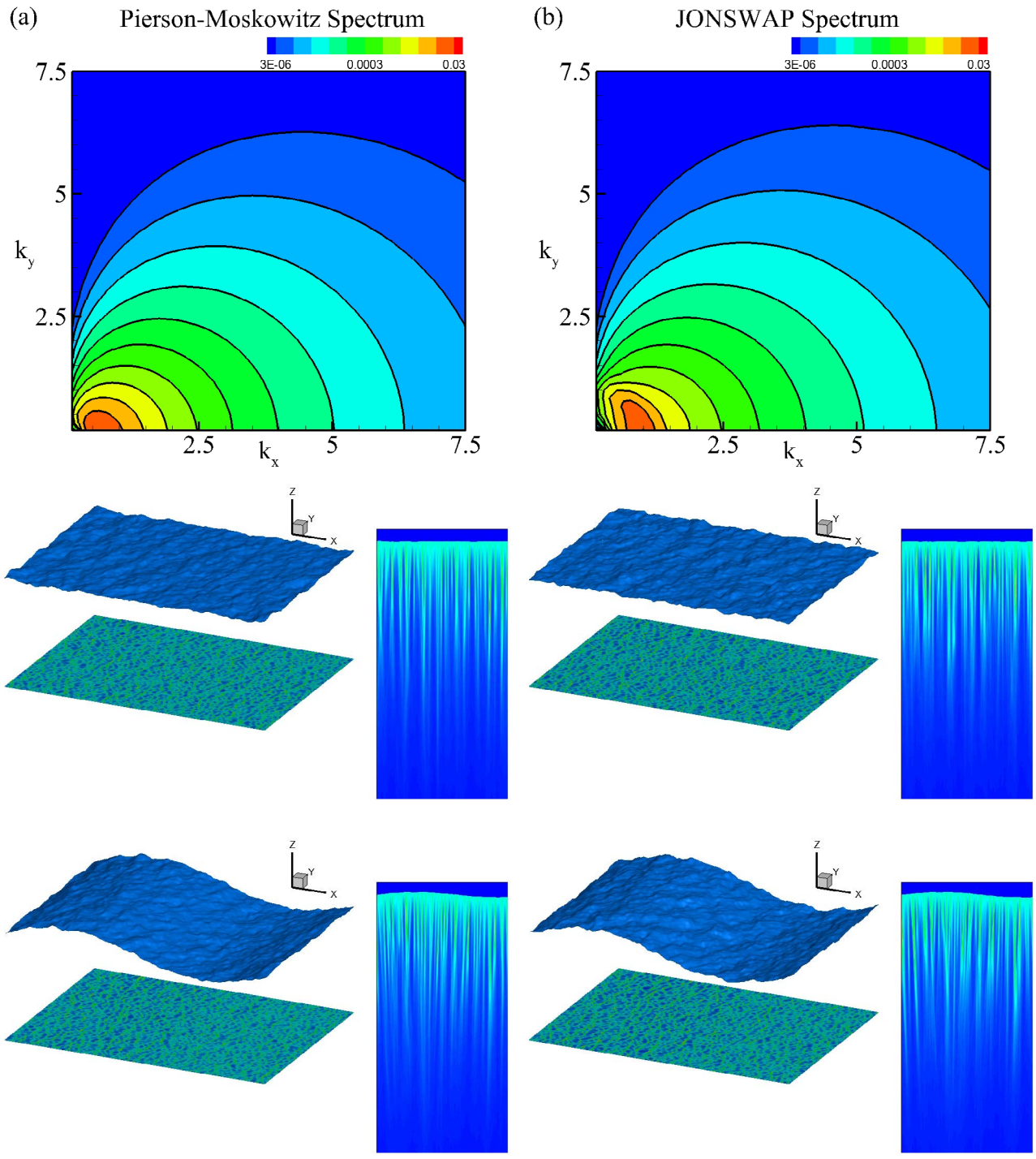

Figure 6. Irradiance field under ocean waves of (a) Pierson-Moskowitz spectrum and (b) JONSWAP spectrum with and without swell. The following are plotted: the spectrum of surface elevation (upper) and surface profiles, horizontal distribution of downwelling irradiance field at representative depths, and vertical distribution of downwelling irradiance field across the ocean surface for case without swell (middle) and case with swell (lower) are shown.